European Review for Medical and Pharmacological Sciences 2019; 23: 8713-8720

MiR-100 suppresses inflammatory activation of microglia and neuronal apoptosis following spinal cord injury *via* TLR4/NF-κB pathway

X.-H. LI, N.-S. FU, Z.-M. XING

Department of Rehabilitation, Liaocheng People's Hospital, Liaocheng, China

Abstract. – OBJECTIVE: This study aims to ascertain the effect of miR-100 on inflammation, apoptosis and functional rehabilitation after spinal cord injury (SCI) and the potential mechanism.

MATERIALS AND METHODS: Firstly, microglia were extracted from 3-day-old neonatal rats and cultured for the purpose of inflammatory activation. Quantitative Real Time-Polymerase Chain Reaction (qRT-PCR) was conducted to detect the levels of miR-100, toll-like receptors 4 (TLR4) and nuclear factor-κB (NF-κB). Moreover, proteins expressions of I-κB and induced-nitric oxide synthase (iNOS) and apoptosis-related genes were measured by Western blotting. In addition, SCI model was established in rats. Expressions of inflammatory factors in SCI rats were determined by enzyme-linked immunosorbent assay (ELISA) assay. Expression levels of TLR4/NF-κB pathway and miR-100 were determined by qRT-PCR. Immunofluorescence was conducted to measure activated microglia. Hindlimbs motor function in SCI rats was estimated *via* BBB 21-point rating scale.

RESULTS: In activated microglia, miR-100 level decreased, while TLR4 and NF-κB levels increased. The protein level of I-κB decreased and iNOS increased. Transfection of miR-100 mimics reversed the above trends. Inflammatory factors were highly elevated in SCI rats and mRNA levels of the TLR4/NF-κB pathway and miR-100 were down-regulated, which were ameliorated in SCI rats overexpressing miR-100 *in vivo*. The amount of activated microglia was declined with the administration of miR-100 mimics compared with the untreated SCI rats. Furthermore, apoptosis-related proteins were down-regulated by miR-100 mimics injection. Motor function in the miR-100 mimics group was improved better than that in the SCI group.

CONCLUSIONS: MiR-100 alleviates inflammation of microglia and neuronal tissue apoptosis, and improves motor function following SCI *via* inhibiting the TLR4/NF-κB pathway.

Key Words:
Spinal cord injury, MiR-100, TLR4/NF-κB pathway, Inflammation and apoptosis.

Introduction

Spinal cord injury (SCI) is a kind of trauma of the central nervous system (CNS) with extremely high disability rate, leading to functional loss of sensory, motor and sphincter. SCI results in paralysis, urinary and fecal dysfunction and other symptoms[1,2]. SCI is divided into primary SCI (PSCI) and secondary SCI (SSCI)[3]. PSCI is caused by the direct or indirect effect of the initial external force on the spinal cord[4]. SSCI is based on the primary injury through a series of pathological processes, where normal tissues around the lesions are impaired and damage area is expanded[5]. Recent studies[6-8] have shown that regulation to inflammation and microenvironment after SCI have advantages on the recovery of neural tissue. The inflammatory response after SCI is mainly regulated by cytokines, chemokines, reactive oxygen species and second messengers secreted by CNS-activated glial cells and peripheral immune cells[9-11]. Immune, biochemical and pathophysiological processes are all involved in the pathogenesis of SCI. The severity depends on primary injury and the pathological process of secondary injury. The acute phase of the inflammatory response is characterized by invasion of neutrophils and monocytes into the damaged area of the spinal cord, while the chronic phase is dominated by mediated lymphocyte[12]. In addition, glial cells rapidly respond to SCI, thus upregulating the expressions of inflammatory factors within a few hours[13-15]. The glial cell population in CNS mainly includes astrocytes,

Corresponding Author: Zhangmin Xing, BM; e-mail: 604353954@qq.com

microglia and oligodendrocytes, contributing to protect neurons and participate in the innate immune response of CNS in normal condition[16-18]. Once SCI occurs, injury-related model molecules, myelin, interferon γ and cell debris are released from damaged tissues or cells, which trigger the activation of microglia cells and lead to morphological and functional changes[19,20]. There are two cell subtypes of microglia, M1 pro-inflammatory phenotype and M2 anti-inflammatory phenotype, which jointly maintain the balance of the spinal cord environment[21,22]. After activation, M1 microglia release pro-inflammatory cytokines and express CD45, CD11b and iNOS, triggering neurotoxic cascade reaction in SSCI that accelerates apoptosis and necrosis of endothelial cells, neurons, axons and oligodendrocytes[23,24]. In contrast, M2 microglia are activated and they release anti-inflammatory cytokines, CD206-mannose-receptor, CD163 scavenger receptor and arginase to protect neurons and axons[25]. Therefore, induction of microglia polarization in a controlled manner is of significance to regulate nerve injury and repair after SCI. The regulatory role of microRNA (MiRNA) in SCI has been reported, which is able to promote the neural repair and functional improvement after SCI[26]. Hu et al[27] demonstrated that miR-126 promotes angiogenesis and attenuates inflammation after spinal cord contusion. Xu et al[28] considered that inhibition of miR-497 reduces inflammation and apoptosis and protects spinal cord ischemia-reperfusion injury. Izumi et al[29] pointed out that miR-223 is upregulated in neutrophils in the early phase of secondary damage after SCI. In the current study, we discovered that miR-100 attenuated inflammatory response and apoptosis by inhibiting the toll-like receptors 4 (TLR4)/nuclear factor-κB (NF-κB) pathway, thus protecting neurons and axons from the invasion of secondary injury.

Materials and Methods

Primary Microglia Culture and Treatment

3-day-old neonatal rats were sacrificed for extracting primary microglia. In brief, the cerebral cortex was harvested and digested in trypsin. After centrifugation and cell separation, the purified microglia were cultured in the Dulbecco's Modified Eagle's Medium (DMEM; Thermo Fisher Scientific, Waltham, MA, USA) containing 10% fetal bovine serum (FBS; Gibco, Grand Island, NY, USA) and 1% streptomycin and penicillin. When cell density reached 95%, cells were induced with 100ng/ml lipopolysaccharide (LPS) for 24 h. The cells in the miR-100 group were pre-transfected with miR-100 mimics for 24 h.

Animals and Grouping

A total of 72 female Sprague Dawley (SD) rats aged 6-8 week and weighted at 200 g-220 g were used for this experiment. All rats were placed in cages and fed with conventional food and water. The breeding environment was maintained at 22-24°C, 50%-55% humidity and 12 h/12 h artificial circadian cycle. Three groups (Sham group, SCI group, miR-100 group) were established for *in vivo* experiment. Rats in the Sham group were only conducted laminectomy. Rats in the SCI group were conducted SCI modeling and injected the same amount of normal saline intrathecally in the damaged site. Rats in the miR-100 group were conducted SCI modeling and injected with miR-100 mimics intrathecally. This study was approved by the Animal Ethics Committee of Liaocheng People's Hospital University Animal Center.

Operative Procedure and Treatment

Initially, rats were anesthetized with 10% paraformaldehyde at 4 mL/kg, followed by skin disinfection at the operation area. After localization of the T10 spinous process, the fascia and muscle tissues were separated for exposure of T10 lamina. Laminectomy was carried out and the spinal cord was exposed. ALLEN bump equipment (10 g × 5 cm) was used to damage spinal cord tissue. Successful spinal cord injury modeling exhibited that rats suffered from spinal cord hemorrhage and delayed extension of hindlimbs and tail swing. Rats in the miR-100 group received an intrathecal injection of miR-100 mimics. Auxiliary urination was conducted three times a day until the urination reflex was recovered.

Western Blotting

Spinal cord tissue or microglia were lysed on ice using a total protein extraction kit containing protease inhibitors and phosphatase inhibitors for protein extraction. Protein mixture was centrifuged at 4°C, 13000 rpm for 15 minutes. The concentration of proteins was measured by double bicinchoninic acid (BCA) method (Beyotime, Shanghai, China). An equal amount of proteins were subjected to electrophoresis in 10% sodium dodecyl sulfate-polyacrylamide gel. Then the dispersed proteins were transferred on polyvi-

nylidene difluoride (PVDF) membranes (Millipore, Billerica, MA, USA) at 4°C. 5% non-fatty milk was prepared with Tris-Buffered Saline with Tween 20 (TBST; Sigma-Aldrich, St. Louis, MO, USA) to block the non-specific antigen for 1 h at room temperature. After washing with TBST three times, the membrane was incubated with primary antibody iNOS (Abcam, Cambridge, MA, USA), Rabbit, 1:250; I-κB (Abcam, Cambridge, MA, USA), Rabbit, 1:1000; caspase-3 (Abcam, Cambridge, MA, USA), Rabbit, 1:1000; caspase-8, (Abcam, Cambridge, MA, USA), Rabbit, 1:1000; caspase-9 (Abcam, Cambridge, MA, USA), Rabbit, 1:1000; bcl-2 (Abcam, Cambridge, MA, USA), Rabbit, 1:1000; GAPDH (Proteintech, Rosemont, IL, USA, 1:10000) at 4°C overnight. On the next day, membranes were incubated with the secondary antibody (Goat Anti-Rabbit IgG, YiFeiXue Biotechnology, Nanjing, China, 1:3000) at room temperature for 1 h and washed 3 times again. Enhanced chemical luminescence (ECL; Thermo Fisher Scientific, Waltham, MA, USA) was used to display the target protein on an exposure machine.

Quantitative Real Time-Polymerase Chain Reaction (qRT-PCR)

Spinal cord tissues or cells were lysed in 1 mL of TRIzol (Invitrogen, Carlsbad, CA, USA) on ice. 0.2 ml of chloroform was added into every 1 mL of TRIzol, and the mixture was violently shaken for 15 seconds and left at room temperature for 3 minutes. The mixture was centrifuged for 15 minutes (10000 RPM, 4°C) and then the upper water phase was collected for incubation with isopropanol. The mixture was vibrated and placed at room temperature for 10 minutes. After the mixture has been centrifuged for 10 minutes (10000 RPM, 4°C), RNA precipitation was collected, washed with 75% ethanol and centrifuged (10000 RPM, 4°C) for 5 minutes. The supernatant was removed and 30 μL of RNase-free water was added to dissolve it. RNA concentrations were measured on NanoDrop to determine the absorbance at 260 nm, 230 nm and 280 nm. RNA with 1.8-2.0 of A260/A280 was considered to be qualified for subsequent experiments.

Quantitative Real Time-Polymerase Chain Reaction was performed using the Prism 7300 Sequence Detection System (Applied Biosystems, Foster City, CA, USA). 25 μL of the reaction system was prepared, including SYBR Green (12.5 μL), 10 mM of primers (0.5 mL each from the stock), 10.5 μL of water and 0.5 μL of the template. The PCR conditions were as follows: 10 min denaturation at 95°C; 40 cycles of denaturation at 95°C for 15 s, 60°C annealing for 30 s and 72°C extension for 30 s. Endogenous GAPDH was used to standardize the data. The comparative threshold cycle (Ct) method, that was the $2^{-\Delta\Delta Ct}$ method, was used to calculate fold amplification. Primer sequences used in this study were as follows: TLR4, F: 5'-CTTAGGAAGGCATCCTTAACTC-3', R: 5'-CGGTAGGATGTCCCGACAGTGA-3'; microRNA-100, F: 5'-GGCTTGTAACCATCCAAGACTG-3', R: 5'-GCATCGCGAATCGTCGAGCCG-3'; NF-κB, F: 5'-ATGCACCGCGGCATATTACAA-3', R: 5'-CAGTGAGAATACGAACATCT-3'; U6: F: 5'-GCTTCGGCAGCACATATACTAAAAT-3', R: 5'-CGCTTCAGAATTTGCGTGTCAT-3'; GAPDH: F: 5'-CGCTCTCTGCTCCTCCTGTTC-3', R: 5'-ATCCGTTGACTCCGACCTTCAC-3'.

Enzyme-Linked Immunosorbent Assay

Spinal cord samples were taken from rats. After adding an appropriate amount of Phosphate-Buffered Saline (PBS; Gibco, Grand Island, NY, USA) to clean the tissue, the mixture was homogenized and centrifuged for 10 minutes to collect the supernatant. Standard product wells are set on the 96-well plate and standard products of different concentrations were added successively. The samples to be tested were added into the corresponding wells, and then the plates were sealed with the sealing film and incubated at room temperature for 30 minutes. Cells were washed using a washing solution for 30 seconds and repeated 5 times. The enzyme standard reagent was added into each well, except blank wells. The colorant was added into each well and cultured in the dark for 15 minutes. The termination solution was added to terminate the reaction and the absorbance (OD value) of each well was measured sequentially at the wavelength of 450 nm by zeroing in the blank hole. With the concentration of standard product as the abscissa and OD value as the ordinate, the standard curve was drawn to calculate the sample concentration.

Immunofluorescence

Rat spinal cord samples were placed in the 4% paraformaldehyde to immobilization for 24 h. Tissues were dehydrated under different concentration sucrose solutions, embedded in OCT and cut into 10 μm sections with a rotary micro-

tome. The rabbit serum was utilized to block the non-specific antigens at room temperature for 1 h. Washed by PBS, the sections were incubated with the primary antibodies IBA-1 (Abcam, Cambridge, MA, USA), Rabbit, 1:300; iNOS (Abcam, Cambridge, MA, USA), Rabbit, 1:100; NF 200 (Cell Signaling Technology, Danvers, MA, USA), Rabbit, 1:200 at 4°C overnight. On the next day, sections were incubated with fluorescent secondary antibodies in the dark for 2 h. Nucleus was stained by 4',6-diamidino-2-phenylindole (DAPI) Fluoromount-G (Sigma-Aldrich, St. Louis, MO, USA) and sections were sealed for 5 min. The sections were visualized using a fluorescence microscope.

Behavioral Assessment

Basso-Beattie-Bresnahan (BBB) locomotor rating scale was used to evaluate the recovery of locomotor coordination function of hindlimbs within four weeks following SCI. Two blinded experimenters scored the rats on a scale of 0 to 21 as they observed their movements in an open field. The evaluation was conducted at 1, 7, 14, 21, and 28 days after SCI modeling.

Statistical Analysis

Statistical Product and Service Solutions (SPSS) 16.0 (SPSS, Chicago, IL, USA) software was used to analyze the experimental data. Measurement data were expressed as $\bar{x} \pm s$. The *t*-test was used for comparisons between the two groups. Single-factor analysis of variance (ANOVA) was used for the comparison between groups with different concentrations. Least Significant Difference (LSD) test or Student-Newman-Keuls (SNK) test was used for pairwise comparison under the condition of homogeneity of variance. Test level α=0.05. All experiments were repeated 3 times.

Results

Transfection of MiR-100 in Microglia Alleviated Inflammatory Activation by Inhibiting the TLR4/NF-κB Pathway

To explore the role of miR-100 in glial inflammation, we firstly transfected miR-100 mimics in LPS-induced microglia. MiR-100 level in microglia treated with LPS only decreased compared with the control group, which was rescued by pre-transfection of miR-100 mimics. Moreover, TLR4 and NF-κB were up-regulated in LPS-induced microglia, which were down-regulated in those pre-transfected with miR-100 mimics (Figure 1A). I-κB, a restraining functional protein to NF-κB and inflammatory microglia biomarker iNOS were measured by Western blotting (Figure 1B). The result exhibited that I-κB expression was elevated and the iNOS level was declined by overexpression of miR-100. Hence, miR-100 alleviated inflammation in microglial by inhibiting the TLR4/NF-κB pathway.

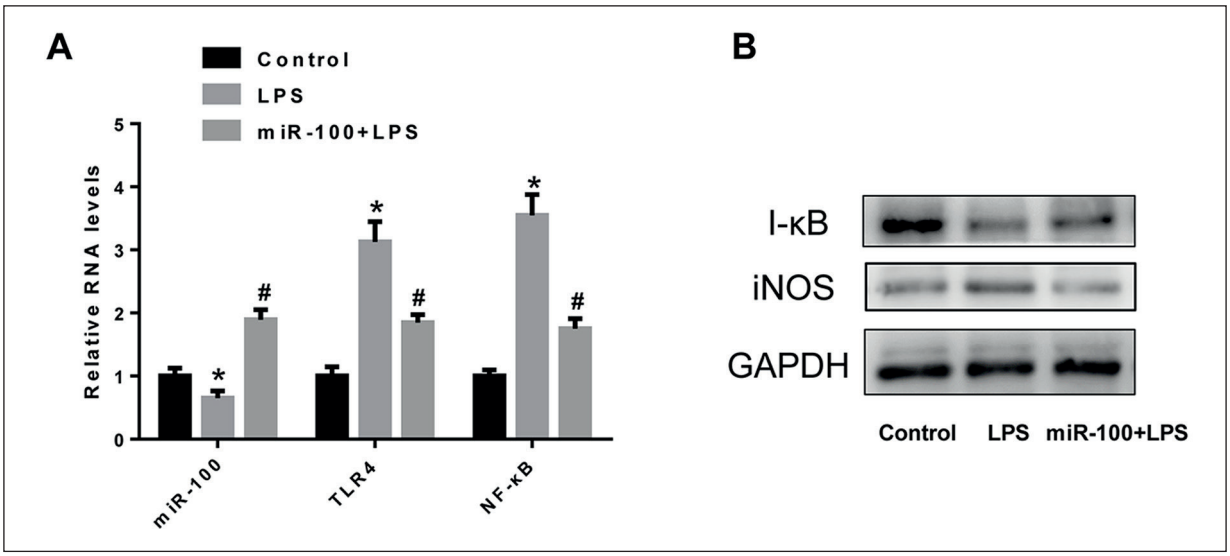

Figure 1. Transfection of miR-100 mimics in microglia decreased inflammatory activation by inhibiting the TLR4/NF-κB pathway. **A,** RNA levels of miR-100, TLR4 and NF-κB *in vitro*. **B,** Protein expressions of I-κB and iNOS *in vitro*.

Increased MiR-100 Ameliorated Inflammation Response via Suppressing the TLR4/NF-κB Pathway Following SCI

In SCI rats, miR-100 level gradually decreased within one week following the injury. Subsequently, TLR4 and NF-κB levels in rats of each group were monitored, which were upregulated in SCI rats. SCI rats overexpressing miR-100 had lower levels of TLR4 and NF-κB (Figure 2A). In addition, inflammatory factors within one week after injury were measured with enzyme-linked immunosorbent assay (ELISA), showing lower levels of tumor necrosis factor alpha (TNF-α), interleukin-6 (IL-6) and monocyte chemoattractant protein-1 (MCP-1) in the miR-100 group compared with those in the SCI group (Figure 2B). The amount of activated microglia was visualized using immunofluorescent staining, displaying a decline in inflammatory microglia around the injury site at 3 days following SCI in the miR-100 group (Figure 2C). All results exhibited that miR-100 overexpression suppressed the TLR4/NF-κB pathway, inflammation and microglia activation.

Treatment of MiR-100 Inhibited Apoptosis and Rescued the Account of Neurofilaments After SCI

Furthermore, we detected apoptosis-related proteins at 7 days after SCI, showing that the miR-100 down-regulated caspase-3, caspase-8 and caspase-9, but Bcl-2, an anti-apoptotic factor was up-regulated (Figure 3A). In addition, we exhibited the account of neurofilaments using immunofluorescent staining (Figure 3B). The result displayed that the number of neurofilaments increased after miR-100 overexpression. Hence, miR-100 inhibited apoptosis and protected neurofilaments *via* down-regulating the TLR4/ NF-κB pathway after SCI.

MiR-100 Administration Improved Hindlimbs Function Recovery After SCI in Rats

Hindlimbs function of rats was assessed by BBB rating scale within four weeks after modeling. There was no abnormal locomotor function in rats of the Sham group. However, rats in the other two groups developed severe hindlimbs dysfunction after modeling. Until two weeks af-

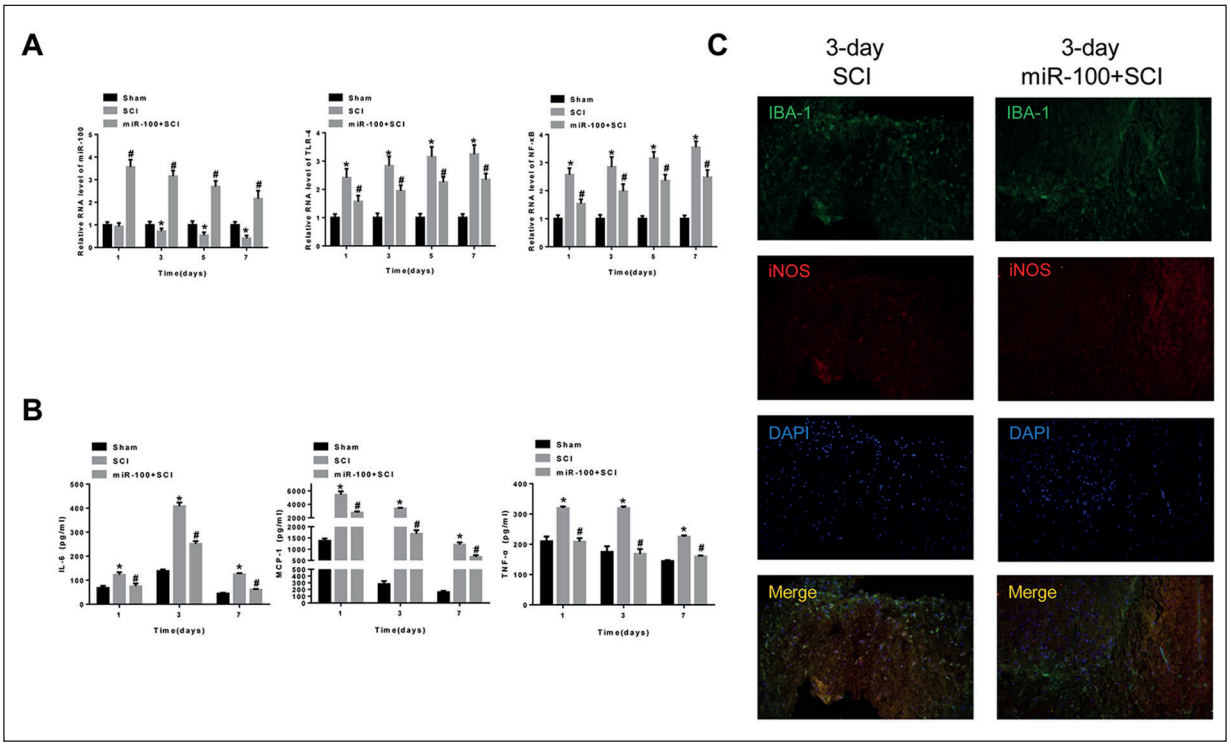

Figure 2. Increased miR-100 ameliorated inflammation response *via* suppressing the TLR4/NF-κB pathway following SCI. **A,** RNA levels of miR-100, TLR4 and NF-κB during one week after SCI. **B,** IL-6, MCP-1 and TNF-α contents in injured spinal cord tissues during one week following injury. **C,** Immunofluorescence co-staining of microglia cell marker (IBA-1) and inflammatory microglia marker (iNOS) in spinal cord tissue at 3 days post-SCI (magnification × 40).

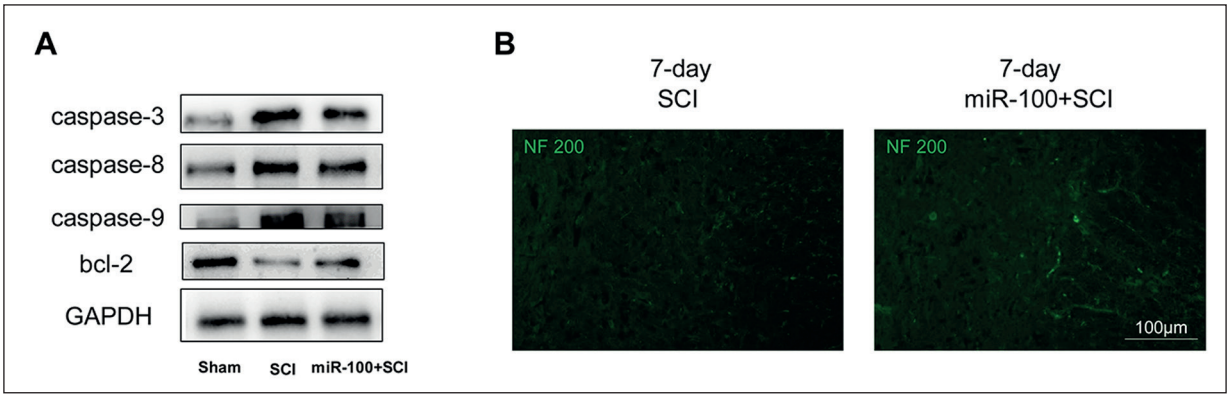

Figure 3. Overexpression of miR-100 inhibited apoptosis and rescued the account of neurofilaments after SCI. **A,** Protein expressions of caspase-3, caspase-8, caspase-9 and Bcl-2 in injured spinal cord at 7 days. **B,** Immunofluorescence staining of neurofilaments marker (NF-200) in damaged spinal cord at 7 days after SCI (magnification × 40).

ter injury, the recovery of the hindlimbs movement of rats overexpressing miR-100 significantly improved compared with those in the SCI group. The difference was the most significant at 28 days (Figure 4). The results of the BBB rating scale demonstrated that overexpression of miR-100 was instrumental in ameliorating the recovery of hindlimbs functions in rats after SCI.

Discussion

At post-SCI, microglia activation induces neural tissue inflammation and activation of inflammatory factors, therefore triggering neural tissue

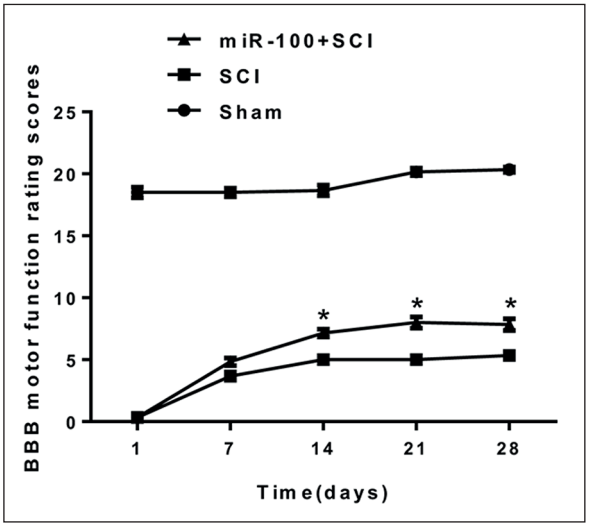

Figure 4. MiR-100 administration improved hindlimbs function recovery after SCI in rats. The scores evaluated by BBB rating scale of three groups during four weeks after SCI.

apoptosis, neuron loss and neural dysfunction[30]. Microglia decrease the phagocytosis, a large number of cytotoxic substances are produced, such as interleukin-1, interferon γ, IL-6, TNF and other pro-inflammatory factors, which promote nitric oxide and reactive oxygen species, functioning toxic effects on neurons and other glial cells[31]. TLR4 is one of the important receptors for microglia activation and function. After CNS injury, expressions of TLR4 and NF-κB were up-regulated and the secretion of downstream inflammatory cytokines was stimulated[32,33]. NF-κB is a pleiotropic transcription factor found in almost all cell types. The NF-κB/Rel family consists of five members: Rel (cRel), p65 (RelA/NF-κB3), RelB, p50, and p52 (NF-κB2), all of which are characterized by a highly conserved Rel homologous domain consisting of 300 amino acids[34]. This region contains DNA binding, dimerization, I-κB interaction and nuclear localization signal region. Homologous or heterodimers can be formed between NF-κB/Rel family members, most commonly with p65 or p50. NF-κB, as a key signal transduction factor, plays a central role in the inflammatory response and inflammation deterioration induced by inflammatory cytokines, chemokines and adhesion molecules[35]. In this study, we certified the anti-inflammation function of miR-100 in SCI by inhibiting the TLR4/NF-κB pathway. Moreover, miR-100 rescued neurons and axons by down-regulating apoptosis-related proteins and improved hindlimbs motor function after SCI. The control of inflammatory level after SCI has always been an important treatment method to maintain the integrity of nerve structure and promote the re-

covery of nerve function. Short-term control of inflammation expansion and secondary injury by inflammation are important for the repair of nerve tissue, which can reduce the neurotoxicity of inflammatory microglia cells. Overexpression of miR-100 alleviated inflammatory response and improved motor function following SCI. Our findings provide new directions in the treatment of SCI.

Conclusions

MiR-100 inhibited inflammation of microglia, reduced neural tissue apoptosis and improved motor function at post-SCI by down-regulating the TLR4/NF-κB pathway.

Conflict of Interest

The Authors declare that they have no conflict of interests.

References

1) Dubreuil CI, Winton MJ, McKerracher L. Rho activation patterns after spinal cord injury and the role of activated Rho in apoptosis in the central nervous system. J Cell Biol 2003; 162: 233-243.
2) Lin XY, Lai BQ, Zeng X, Che MT, Ling EA, Wu W, Zeng YS. Cell transplantation and neuroengineering approach for spinal cord injury treatment: a summary of current laboratory findings and review of literature. Cell Transplant 2016; 25: 1425-1438.
3) Amar AP, Levy ML. Pathogenesis and pharmacological strategies for mitigating secondary damage in acute spinal cord injury. Neurosurgery 1999; 44: 1027-1039, 1039-1040.
4) Werndle MC, Saadoun S, Phang I, Czosnyka M, Varsos GV, Czosnyka ZH, Smielewski P, Jamous A, Bell BA, Zoumprouli A, Papadopoulos MC. Monitoring of spinal cord perfusion pressure in acute spinal cord injury: initial findings of the injured spinal cord pressure evaluation study. Crit Care Med 2014; 42: 646-655.
5) Cohen TI, Weinberg RJ, Blight AR. Intrathecal infusion of the nitric oxide synthase inhibitor N-methyl L-arginine after experimental spinal cord injury in guinea pigs. J Neurotrauma 1996; 13: 361-369.
6) Yuan Y, Su Z, Pu Y, Liu X, Chen J, Zhu F, Zhu Y, Zhang H, He C. Ethyl pyruvate promotes spinal cord repair by ameliorating the glial microenvironment. Br J Pharmacol 2012; 166: 749-763.
7) Radulovic M, Yoon H, Wu J, Mustafa K, Scarisbrick IA. Targeting the thrombin receptor modulates inflammation and astrogliosis to improve recovery after spinal cord injury. Neurobiol Dis 2016; 93: 226-242.
8) Donnelly DJ, Longbrake EE, Shawler TM, Kigerl KA, Lai W, Tovar CA, Ransohoff RM, Popovich PG. Deficient CX3CR1 signaling promotes recovery after mouse spinal cord injury by limiting the recruitment and activation of Ly6Clo/iNOS+ macrophages. J Neurosci 2011; 31: 9910-9922.
9) Gwak YS, Kang J, Unabia GC, Hulsebosch CE. Spatial and temporal activation of spinal glial cells: role of gliopathy in central neuropathic pain following spinal cord injury in rats. Exp Neurol 2012; 234: 362-372.
10) Kubota K, Saiwai H, Kumamaru H, Maeda T, Ohkawa Y, Aratani Y, Nagano T, Iwamoto Y, Okada S. Myeloperoxidase exacerbates secondary injury by generating highly reactive oxygen species and mediating neutrophil recruitment in experimental spinal cord injury. Spine (Phila Pa 1976) 2012; 37: 1363-1369.
11) Ghirnikar RS, Lee YL, Eng LF. Chemokine antagonist infusion attenuates cellular infiltration following spinal cord contusion injury in rat. J Neurosci Res 2000; 59: 63-73.
12) Tator CH, Fehlings MG. Review of the secondary injury theory of acute spinal cord trauma with emphasis on vascular mechanisms. J Neurosurg 1991; 75: 15-26.
13) Tzeng SF, Bresnahan JC, Beattie MS, de Vellis J. Upregulation of the HLH Id gene family in neural progenitors and glial cells of the rat spinal cord following contusion injury. J Neurosci Res 2001; 66: 1161-1172.
14) Tauchi R, Imagama S, Ohgomori T, Natori T, Shinjo R, Ishiguro N, Kadomatsu K. ADAMTS-13 is produced by glial cells and upregulated after spinal cord injury. Neurosci Lett 2012; 517: 1-6.
15) Han X, Yang N, Xu Y, Zhu J, Chen Z, Liu Z, Dang G, Song C. Simvastatin treatment improves functional recovery after experimental spinal cord injury by upregulating the expression of BDNF and GDNF. Neurosci Lett 2011; 487: 255-259.
16) Kahn MA, Kumar S, Liebl D, Chang R, Parada LF, De Vellis J. Mice lacking NT-3, and its receptor TrkC, exhibit profound deficiencies in CNS glial cells. Glia 1999; 26: 153-165.
17) Xiao BG, Bao WJ, Bai XF, Link H. Induction of cytolysin mRNA in glial cells by IFN-gamma: a possible cytotoxic pathway in the CNS. Neuroreport 1996; 8: 329-333.
18) Ahmed S, Gull A, Khuroo T, Aqil M, Sultana Y. Glial cell: a potential target for cellular and drug based therapy in various CNS diseases. Curr Pharm Des 2017; 23: 2389-2399.
19) Wang X, Cao K, Sun X, Chen Y, Duan Z, Sun L, Guo L, Bai P, Sun D, Fan J, He X, Young W, Ren Y. Macrophages in spinal cord injury: phenotypic and functional change from exposure to myelin debris. Glia 2015; 63: 635-651.

20) Ankeny DP, McTigue DM, Jakeman LB. Bone marrow transplants provide tissue protection and directional guidance for axons after contusive spinal cord injury in rats. Exp Neurol 2004; 190: 17-31.

21) Habib P, Slowik A, Zendedel A, Johann S, Dang J, Beyer C. Regulation of hypoxia-induced inflammatory responses and M1-M2 phenotype switch of primary rat microglia by sex steroids. J Mol Neurosci 2014; 52: 277-285.

22) Michelucci A, Heurtaux T, Grandbarbe L, Morga E, Heuschling P. Characterization of the microglial phenotype under specific pro-inflammatory and anti-inflammatory conditions: effects of oligomeric and fibrillar amyloid-beta. J Neuroimmunol 2009; 210: 3-12.

23) Woo MS, Park JS, Choi IY, Kim WK, Kim HS. Inhibition of MMP-3 or -9 suppresses lipopolysaccharide-induced expression of proinflammatory cytokines and iNOS in microglia. J Neurochem 2008; 106: 770-780.

24) Nayak D, Huo Y, Kwang WX, Pushparaj PN, Kumar SD, Ling EA, Dheen ST. Sphingosine kinase 1 regulates the expression of proinflammatory cytokines and nitric oxide in activated microglia. Neuroscience 2010; 166: 132-144.

25) Tang Y, Le W. Differential roles of M1 and M2 microglia in neurodegenerative diseases. Mol Neurobiol 2016; 53: 1181-1194.

26) Liu NK, Wang XF, Lu QB, Xu XM. Altered microRNA expression following traumatic spinal cord injury. Exp Neurol 2009; 219: 424-429.

27) Hu J, Zeng L, Huang J, Wang G, Lu H. MiR-126 promotes angiogenesis and attenuates inflammation after contusion spinal cord injury in rats. Brain Res 2015; 1608: 191-202.

28) Xu M, Wang HF, Zhang YY, Zhuang HW. Protection of rats spinal cord ischemia-reperfusion injury by inhibition of MiR-497 on inflammation and apoptosis: possible role in pediatrics. Biomed Pharmacother 2016; 81: 337-344.

29) Izumi B, Nakasa T, Tanaka N, Nakanishi K, Kamei N, Yamamoto R, Nakamae T, Ohta R, Fujioka Y, Yamasaki K, Ochi M. MicroRNA-223 expression in neutrophils in the early phase of secondary damage after spinal cord injury. Neurosci Lett 2011; 492: 114-118.

30) Tian DS, Xie MJ, Yu ZY, Zhang Q, Wang YH, Chen B, Chen C, Wang W. Cell cycle inhibition attenuates microglia induced inflammatory response and alleviates neuronal cell death after spinal cord injury in rats. Brain Res 2007; 1135: 177-185.

31) Sugama S, Cho BP, Degiorgio LA, Shimizu Y, Kim SS, Kim YS, Shin DH, Volpe BT, Reis DJ, Cho S, Joh TH. Temporal and sequential analysis of microglia in the substantia nigra following medial forebrain bundle axotomy in rat. Neuroscience 2003; 116: 925-933.

32) Bauman TM, Becka AJ, Sehgal PD, Huang W, Ricke WA. SIGIRR/TIR8, an important regulator of TLR4 and IL-1R-mediated NF-kappaB activation, predicts biochemical recurrence after prostatectomy in low-grade prostate carcinomas. Hum Pathol 2015; 46: 1744-1751.

33) Shah VB, Williams DL, Keshvara L. beta-Glucan attenuates TLR2- and TLR4-mediated cytokine production by microglia. Neurosci Lett 2009; 458: 111-115.

34) Hernandez-Gutierrez S, Garcia-Pelaez I, Zentella-Dehesa A, Ramos-Kuri M, Hernandez-Franco P, Hernandez-Sanchez F, Rojas E. NF-kappaB signaling blockade by Bay 11-7085 during early cardiac morphogenesis induces alterations of the outflow tract in chicken heart. Apoptosis 2006; 11: 1101-1109.

35) Tak PP, Firestein GS. NF-kappaB: a key role in inflammatory diseases. J Clin Invest 2001; 107: 7-11.